ISSN 0915-633X

NATIONAL INSTITUTE FOR FUSION SCIENCE

Anomalous Cross Field Flux in CHS

T. Yamagishi

(Received – Apr. 28, 1993)

NIFS-227 May 1993

RESEARCH REPORT
NIFS Series

NAGOYA, JAPAN

Anomalous Cross Field Flux in CHS

T.Yamagishi
Fukui Institute of Technology
Gakuen Fukui 910

Abstract

Anomalous quasi-linear fluxes induced by the curvature drift resonance and transit resonace are evaluated in a rotating helical plasma. The radial electric field makes the Doppler shift, but does not contribute to the anomalous fluxes. The curvature drift resonance induces the new curvature term in the quasi-linear fluxes. The effect of helical magnetic field is through this curvature of magnetic field lines, and contributes to the inward transport. The ion heat diffusivity due to the curvature drift resonance is obtained in the form of modified gyro-Bohm coefficient, and is compared with experimentally observed one in CHS Heliotron.

Keywords: Radial electric field, cross field fluxes, curvature drift resonance continuum, transit resonance continuum. ion heat diffusivity, inward transport due to curvature drift, trapped electron curvature drift resonance, modified gyro-reduced Bohm coefficient, comparision of experimental results in CHS Heliotron,

§1. Introduction

Transport coefficients observed in Tokamaks(1) and Heliotron /Torsatron(2) are larger than those coefficients predicted by neoclassical theory more than one order of magnitude. Anomalous transport phenomena seem to dominate the plasma transport processes in various toroidal confinement fusion devices.

The anomalous transport coefficients are usually evaluated by assuming the existence of certain micro-instability, i.e., the existence of unstable discrete time eigenvalue. In addition to the discrete eigenvalue, the basic Vlasov equation has the continuous eigenvalue(3)(4) induced by the wave-particle resonance condition. Although this continuous eigenvalue does not affect the instability or the discrete eigen mode, it contributes to the plasma transport.

In a pevious report(5)(6), the effect of continuous eigenvalue on ion transport has been studied, and successfully interpreted the experimentally observed phenomenon in a tokamak. In this report, we will apply the same theory to the interpretation of experimentally observed transport coefficients in CHS Heliotron.

In the toroidal coordinate system (r,θ,φ), the magnetic field in the toroidal-helical configuration is given by $B=Bo(1-\varepsilon_t\cos\theta-\varepsilon_h\cos(l\theta-m\varphi))$. In the CHS Heliotron, the toroidal effect $\varepsilon_t=r/R_o$ is smaller than the helical effect $\varepsilon_h=\varepsilon_o I_l(mr/R_o)$ except near the plasma center region, where I is the modified Bessel function. We consider, therefore, the helically symmetric system neglecting the toroidal effect. This helical magnetic field may modifies the equilibrium distribution by the neoclassical effect. For the sake of simplicity, we will neglect this effect, and consider the Maxwellian plasma. The helical magnetic field modifies the particle motion through the curvature drift and the local magnetic mirror effect. We will take into account these helical effects in evaluating the continuum contributions for the quasi-linear electron, ion and energy fluxes. The curvature drift effect induces an inward transport term in the fluxes. It, however, does not affect the diffusion and heat diffusivity coefficients.

§2. Cross Field Ion Fluxes

We start with the gyrokinetic solution which includes the effect of electric potential Φ:

$$\tilde{f}=\frac{\omega+\omega_E-\omega_{*T}}{\omega+\omega_E-\omega_D-k_\parallel v_\parallel}J_o^2(\alpha)F_M\frac{e\tilde{\phi}}{T} \quad (1)$$

where $\omega_E=k_\theta V_E$ with $V_E=cE_r/B$, $E_r=-\Phi'$, and other notations are standard as defined in Ref.(6). We assume the helical effect is in the precessional drift frequency;

$$\omega_D=\frac{1}{\Omega}\mathbf{b}\times\left(\frac{v_\perp^2}{2}\nabla\ln B+v_\parallel^2\mathbf{k}\right).\nabla S \quad (2)$$

where S is the eikonal. For the low-β plasmas($\beta<<1$), $\kappa=(\mathbf{b}.\nabla)\,\mathbf{b}\cong\nabla\ln B$, we have $\omega_D\cong\hat{\omega}_D(v_\perp{}^2/2+v_\parallel{}^2)$ with $\hat{\omega}_D=2\varepsilon_n\omega_*=cTk_\theta/eBL_B$, $\varepsilon_n=L_n/L_B$, $1/L_n=-d\ln n/dr$ and $1/L_B=-d\ln B/dr$. In the toroidal-helical configuration, the equilibrium distribution may be modified by the neoclassical effect. For the sake of simplicity, however, we will take the lowest order Maxwellian distribution: $F_M=(\pi v_{th})^{-3/2}\exp(-E/T)$ with $E=Mv^2/2+e\Phi$.

We calculate the quasi-linear flux defined by[7]

$$\Gamma=\int d^3v\left\langle\tilde{v}_x\tilde{f}\right\rangle \quad (3)$$

where the angular brackets means the ensemble average for the fluctuations and $\tilde{v}_x=-ik_\theta c\hat{\phi}/B$ is the perturbed radial component of the ExB drift velocity. Substitution of eq.(1) into eq.(3) yields

$$\Gamma=\sum_{k,\omega}\frac{cT}{eB}k_\theta\left|\frac{e\tilde{\phi}}{T}\right|^2_{k\omega}\phi_o(k,\omega) \quad (4)$$

where the normalized flux is defined by

$$\phi_j(k,\omega)=-\mathrm{Im}\int d^3v\frac{\bar{\omega}-\omega_*(1+\eta(\bar{E}-\frac{3}{2}))}{\bar{\omega}-\omega_D-k_\parallel v_\parallel}\bar{E}^jF_MJ_o^2(\alpha) \quad (5)$$

$\bar{\omega}=\omega+\omega_E$ and $\bar{E}=E/T$. By the same manner, the energy flux

$$Q=\int d^3v\left\langle\tilde{v}_x\tilde{f}E\right\rangle \quad (6)$$

can be expressed in the form

$$Q=\sum_{k,\omega}\frac{cT}{eB}k_\theta\left|\frac{e\tilde{\phi}}{T}\right|^2_{k\omega}\phi_1(k,\omega) \quad (7)$$

Notice that the numerator in eq.(5) can be written in the form

$$\bar{\omega}-\omega_*\left(1+\eta\left(E-\frac{3}{2}\right)\right)=\omega-\frac{cT}{eB}k_\theta\left(\frac{n'}{n}+\frac{T'}{T}\left(E-\frac{3}{2}\right)+\frac{e\Phi'}{T}\right) \quad (8)$$

where the electric field term comes form the rotation frequency $\omega_E=k_\theta cE_r/B$. Each term in the right hand side of eq.(8) corresponds to Shaing's neoclassical expression(8) although our resonance denominator is different.

When certain instability, for example the η_i-mode, is excited, the flux ϕ_j may be given by the growth rate γ of the unstable discrete eigenvalue $\omega_o=\omega_r+i\gamma$:

$$\phi_j^o=\int d^3v\frac{\gamma(\omega_D+k_\parallel v_\parallel-\omega_{*T})}{(\omega_r-\omega_D-k_\parallel v_\parallel)^2+\gamma^2}J_o^2(\alpha)F_M\bar{E}^j \quad (9)$$

In the CHS, the experimentally observed plasma density and temprature profiles are expressed by(9):

$$n(x)=(n_o-n_b)\frac{1}{g}(1-x^{\alpha_n})^{\beta_n}\left\{1-(1-g)(1-x^{\alpha_n})^{\beta_n-1}\right\}+n_b \quad (10)$$

$$T(x)=(T_o-T_b)(1-x^{\alpha_T})^{\beta_T}+T_b \quad (11)$$

where g has been defined in Ref.(9). The parameters α_n, β_n, n_o, n_b, α_T, β_T, T_o and T_b are all tabulated in Ref.(9) for the low and high density dicharges. The dencity profile is peaked in the periphery which may be one of the characteristics of the CHS plasma. The important profile parameter η=dlnn/dlnT becomes negative in the central region. The η_i-mode may(10), therefore, be stable at least in the central region of CHS. When the discrete mode is stable, the coresponding flux ϕ_j^o should be zero.

Neglecting the transit frequency $k_\parallel v_\parallel=0$, we evaluate the continuum contribution to the flux induced by the curvature drift resonance condition $\omega=\omega_D$, which always exists independently of the discrete mode. We assume the existence of electrostatice fluctuations which may be induced by some instablities such as resistive g-mode(11) and MHD modes or subcritical nonlinear chaos(12).

If we consider passing particle alone, the velocity integral may be written in the form

$$\int d^3vF_M ... = \frac{1}{\sqrt{\pi}}\int_0^{1/(1+\varepsilon)}\frac{d\lambda}{\sqrt{1-\lambda}}\int_0^{\infty}dE\sqrt{E}e^{-E}... = \frac{(1-\sqrt{\varepsilon})}{\sqrt{\pi}}\int_0^{\infty}dE\sqrt{E}e^{-E}... \tag{12}$$

If we assume $\omega_D=\hat{\omega}_D\bar{E}$ as in Ref.(1), applying eq.(12), the flux (9) induced by the resonance condition $\omega=\omega_D$ can be written as

$$\phi_j^c = -2\sqrt{\pi}\,(1-\sqrt{\varepsilon_h})\int_0^{\infty}dE\sqrt{E}e^{-E}\left\{\bar{\omega}-\omega_*\left(1+\eta\left(E-\frac{3}{2}\right)\right)\right\}\delta(\bar{\omega}-\hat{\omega}_D E) \tag{13}$$

If we consider both component $v_\parallel$ and $v_\perp$ in ω_D, $\phi_j{}^C$ may be expressed by the double integral instead of the single integral as in eq.(13), which may only be calculated numerically.

We introduce the frequency power spectrum $S(\omega)$ by

$$\left|\frac{e\tilde{\phi}}{T}\right|^2_{k\omega} = \left|\frac{e\tilde{\phi}}{T}\right|^2_{k} S(\omega) \tag{14}$$

In this case, fluxes given by eqs.(4) and (7) can, respectively, be written in terms of moments I_j:

$$\Gamma = 2\sqrt{\pi}n(1-\sqrt{\varepsilon_h})\sum\frac{cT}{eB}k_\theta\left|\frac{e\tilde{\varphi}}{T}\right|^2_k\left\{(\hat{\omega}_D-\omega_*\eta)I_1-\omega_*\left(1-\frac{3}{2}\eta\right)I_0\right\} \tag{15}$$

$$Q = 2\sqrt{\pi}nT(1-\sqrt{\varepsilon_h})\sum\frac{cT}{eB}k_\theta\left|\frac{e\tilde{\varphi}}{T}\right|^2_k\left\{(\hat{\omega}_D-\omega_*\eta)I_2-\omega_*\left(1-\frac{3}{2}\eta\right)I_1\right\} \tag{16}$$

where the moment integral is defined by

$$I_j = \int dw\,w^{j+1/2}e^{-w}S(\hat{\omega}_D w-\omega_E) \tag{17}$$

From the definitions of ω_D, ω_* and $\omega_*\eta$, eqs.(15) and (16) can be written in the neoclassical forms:

$$\Gamma = 2\sqrt{\pi}n(1-\sqrt{\varepsilon_h})\sum_k\left|\frac{c\tilde{E}_\theta}{B}\right|^2_k\left\{-I_0\frac{n'}{n}-\left(I_1-\frac{3}{2}I_0\right)\frac{T'}{T}+2I_1\frac{B'}{B}\right\} \tag{18}$$

$$Q = 2\sqrt{\pi}nT(1-\sqrt{\varepsilon_h})\sum_k\left|\frac{c\tilde{E}_\theta}{B}\right|^2_k\left\{-I_1\frac{n'}{n}-\left(I_2-\frac{3}{2}I_1\right)\frac{T'}{T}+2I_2\frac{B'}{B}\right\} \tag{19}$$

where the following relation has been used:

$$\left|\frac{cT}{eB}k_\theta\right|^2\left|\frac{e\tilde{\varphi}}{T}\right|_k^2=\left|\frac{c\tilde{E}_\theta}{B}\right|_k^2 \tag{20}$$

Notice that the electric field E_r term disappeared in eqs.(18) and (19). It is involved implicitly in the moment integral in eq.(17). The frequency spectrums $S(\omega)$ in the rotating plasma measured form the labolatory system may also suffer Doppler shift by ω_E. In this case, ω_E in the moment integral (17) may disappear, and we have no electric field effect in eqs.(15) and (16) as in the linear dispersion relation.

The last curvature term $-B'/B$ in eqs.(18) and (19), is the new term. This term comes from the frequency ω term with the curvature drift resonant condition $\omega=\omega_D$. Since the curvature term is negative, it contributes to inward transport.

We now evaluate the moment integrals assuming a simple cut-off frequency spectrum: $S=1/2\omega_s$ for $|\omega|<\omega_s$ with ω_s being the half width of the frequency spectrum. In this case, we have

$$I_j=\int_0^{\omega_s/|\omega_D|}dw\,w^{j+1/2}e^{-w} \tag{21}$$

If we assume that the width is much wider than the curvature drift frequency, $\omega_s>>|\omega_D|$, the moments may be approximated by infinite integral, and yield $I_0=\sqrt{\pi}/2\omega_s$, $I_1=3\sqrt{\pi}/4\omega_s$ and $I_2=15\sqrt{\pi}/8\omega_s$. Introducing these moments into eqs.(18) and (19), we have

$$\Gamma=\sqrt{\pi}n(1-\sqrt{\varepsilon_h})\sum_k\left|\frac{c\tilde{E}_\theta}{B}\right|_k^2\frac{1}{\omega_s}\left(-\frac{n'}{n}+3\frac{B'}{B}\right) \tag{22}$$

$$Q=3\sqrt{\pi}nT(1-\sqrt{\varepsilon_h})\sum_k\left|\frac{c\tilde{E}_\theta}{B}\right|_k^2\frac{1}{\omega_s}\left(-\frac{n'}{n}-\frac{T'}{T}+5\frac{B'}{B}\right) \tag{23}$$

In eq.(22), T' term is exactly canceled out. The helical effects in eqs.(22) and (23), are in the curvature term B'/B and $\sqrt{\varepsilon_n}$. Since diffusion coefficient D is the coefficient of n', it is given by

$$D=\pi(1-\sqrt{\varepsilon_h})\sum_k\left|\frac{c\tilde{E}_\theta}{B}\right|_k^2\frac{1}{\omega_s} \tag{24}$$

The heat diffuscivity χ is the coefficient of nT' in eq.(23), it can be given by

$$\chi = \frac{3}{2}\pi(1-\sqrt{\varepsilon_h})\sum_k \left|\frac{c\tilde{E}_\theta}{B}\right|_k^2 \frac{1}{\omega_s} \qquad (25)$$

If we assume $\omega_s=3\omega_D=6cTk_\theta/eBL_B$, $\rho_i k_\perp=1/5$, $|e\tilde{\phi}/T|\simeq(k_\perp L)^{-1}$ and $L^2=L_T L_B$, bearing in mind the relation (20), we have

$$\chi = \frac{15\pi}{24}(1-\sqrt{\varepsilon_h})\frac{v_i\rho_i^2}{L_T} \qquad (26)$$

where v_i is the ion thermal velocity and L_T is the scale length of temperature gradient defined by $1/L_T=-T'/T$. The assumption $L^2=L_T L_B$ corresponds to the assumption $L^2=L_T R$ in Ref.(10). With this assumption eq.(24) may be proportional to the interchange type driving force $\omega_D\omega_*\eta_i$ due to the η_i-mode.

Equation (26) may be applicable when the trapped particle effect is neglected. For trapped particles, the bounce resonance and the curvature drift resonance may be possible. We neglect the bounce resonance continuum contribution assuming low bounce frequency $\omega_B<<\omega_D$. The heat diffusivity due to the curvature drift resonance for trapped particles may be, by the same manner as in the above for passing particles, given by $\chi\simeq\varepsilon_h^{1/2}v_i\rho_i^2/L_T$. In this case, the trapped particle contribution may be cancelled out in eq.(26), and we have

$$\chi_{i0} = \frac{v_i\rho_i^2}{L_T} = \left(\frac{v_i\rho_i^2}{a}\right)_0 \left(\frac{T(x)}{T_o}\right)^{3/2} \left(\frac{B_0}{B(x)}\right)^2 \frac{a}{L_T} \qquad (27)$$

where $(f)_o$ means the value of f at x=0. We assume $(v_i\rho_i^2/a)_o=1$ m2/sec and plot the profile of χ_{io} by applying eq.(11) and $B(x)=Bo(1-\varepsilon_h(x))$ to eq.(27).

The radial profile of heat conductivity given by eq.(27) is almost determined by the temperature profile. The radial variation of χ_i is presented for various values of the temperature profile parameter β_T in Fig.1 by a surface graphycis for the case of low density case. As seen in Fig.1, χ_i increases monotonically toward the periphery when $\beta_T\lesssim 1$. For the case of high density discharge, the surface graphics of χ_i is similar to Fig.1.

The ion heat conductivity given by eq.(27) is compared with the experimentally measured one denoted by χ_{iexp} for both low and high dendity cases in Fig.2. Since the numerical coefficient in eq.(27)

may depend on many assumptions such as the constant $k_\theta \rho_i$ and L, the numerical coefficient may be considered as an adjustable parameter. The theoretically calculated χ_i is adjusted at the intermediate position to the experimental values in Fig.2. As seen in Fig.2, the modified gyro-reduced Bohm coefficient given by eq.(27) agrees well with experimental results if we choose $\beta_T \lesssim 1$.

§3. Electron Fluxes due to Transit Resonance

We proceed to the evaluation of electron quasi-linear fluxes. For electrons, the transit frequency $\omega_t = k_\parallel v_e$ may be much higher than the drift frequency ω_D, where v_e is the electron thermal velocity: $T_e = M_e v_e^2/2$. As in section 2, the suffix e for electron will be deleted, because of simplicity and all results are essentially applicable also to ions. In the case of electron, the transit resonance $\omega = k_\parallel v_\parallel$ may be more important. From eq.(1) to eq.(9) in §2 are applicable also to the electron transport due to the transit resonance.

The normalized flux for the transit resonance can be written in the form

$$\phi_j^c = \frac{2}{\sqrt{\pi}} \int_0^\infty dx x e^{-x^2} \int_{y > \sqrt{\varepsilon_h} x} dy \left\{ \bar{\omega} - \omega_* \left(1 + \eta \left(x^2 + y^2 - \frac{3}{2} \right) \right) \right\} e^{-y^2} (x^2 + y^2) \delta(\bar{\omega}^2 - \omega_t^2 y^2)$$

Carrying out the integration with respect to y, we have

$$\phi_j^c = 2 \frac{\sqrt{\pi}}{\omega_t} \left\{ K_j \left(\bar{\omega} - \omega_* \left(1 - \frac{3}{2} \eta \right) \right) - \omega_* \eta K_{j+1} \right\} \tag{28}$$

where the moment integral K_j is defined by

$$K_j = \int_{u_1}^{u_2} du u^j e^{-u} \tag{29}$$

Here the the integral limits are $u_1 = (\omega/\omega_t)^2$ and $u_2 = u_1(1 + 1/\varepsilon_h)$. Introducing eq.(28) into eqs. (4) and (7) applying eq. (14), we have the fluxes in the forms:

$$\Gamma = 2\sqrt{\pi} n \sum_k \frac{cT}{eB} \frac{k_\theta}{\omega_t} \left| \frac{e\tilde{\varphi}}{T} \right|_k^2 \int_{-\infty}^\infty d\omega S(\omega) \left\{ K_0 \left(\bar{\omega} - \omega_* \left(1 - \frac{3}{2} \eta \right) \right) - \omega_* \eta K_1 \right\} \tag{30}$$

$$Q = 2\sqrt{\pi} n T \sum_k \frac{cT}{eB} \frac{k_\theta}{\omega_t} \left| \frac{e\tilde{\varphi}}{T} \right|_k^2 \int_{-\infty}^\infty d\omega S(\omega) \left\{ K_1 \left(\bar{\omega} - \omega_* \left(1 - \frac{3}{2} \eta \right) \right) - \omega_* \eta K_2 \right\} \tag{31}$$

If the helical effect is neglected, $u_2 \to \infty$. In this case, $K_{j+1} = u^{j+1} e^{-u_1} + j K_j$. In particular, $K_0 = e^{-u_1}$, $K_1 = e^{-u_1}(u_1 + 1)$ and

$K_2=e^{-u_1}(1+(u_1+1)^2)$. When the spectrum S is even with respect to the Doppler shifted variable $\bar{\omega}$, the frequency term in eqs.(30) and (31) vanishes, because the moment integrals K_j are even. If we consider the frequency range $\omega \approx \omega_* \ll \omega_t$, the electron thermal flux may be approximated in the form

$$Q_e = 2\sqrt{\pi} n T_e \sum_k \frac{cT_e}{eB} \frac{k_\theta}{\omega_{te}} \left|\frac{e\tilde{\varphi}}{T_e}\right|_k^2 \omega_{*e}\left(1+\frac{\eta_e}{2}\right) \qquad (32)$$

In view of the relation (20), eq.(32) can be written in the neoclassical form

$$Q_e = 2\sqrt{\pi} n T_e \sum_k \left|\frac{c\tilde{E}_\theta}{B}\right|_k^2 \frac{1}{\omega_{te}}\left(-\frac{n'}{n}-\frac{1}{2}\frac{T_e'}{T_e}\right) \qquad (33)$$

Notice that the electric field term disappeared in eq.(33) by the same reason as discussed in section 2.
Applying the same assumptions for fluctuations as in section 2: $|c\tilde{E}_\theta/B|^2=\rho_i^2 v_i^2/4L_BL_T$, from the coefficent of T'_e in eq.(33) we have the electron heat conductivity

$$\chi_e = \frac{\sqrt{\pi}}{2} q \sqrt{\frac{m_e}{m_i}} \chi_i \qquad (34)$$

where χ_i has been given by eq.(26) , $\tau=T_e/T_i$ and $q=2\pi/\iota$ is the safety factor.

Due to the factor of mass ratio, the electorn heat diffusivity χ_e given by eq.(34) induced by the transit resonance continuum is much smaller than χ_i given by eq.(26), and may be neglected as compared with the ion heat diffusivity. The smallness of χ_e given by eq.(34) is due to the smallness of the perturbed distribution for the circulating electrons: $\tilde{f}_e \cong 0(\omega_*/\omega_{te})$.

§4 Trapped Electron Contribution

We now consider the quasi-linear fluxes induced by electrons trapped in the helical magnetic field. The non-adiabtic portion of the trapped particle distribution is given by

$$\tilde{f}_e = \frac{\bar{\omega}-\omega_{*Te}}{\bar{\omega}-\omega_{De}+i\nu_{eff}} F_M \frac{e\tilde{\varphi}}{T_e} \qquad (35)$$

where the electron collision frequency for trapped particle is given by $\nu_{eff}=\nu_e/\epsilon_h$. In this case, the normalized flux defined by eq.(5) is written by

$$\phi_j = \int_T d^3v \frac{\nu_{eff}(\omega_D - \omega_{*T})}{(\overline{\omega}_r - \omega_D)^2 + \nu_{eff}^2} F_M \overline{E}^j \tag{36}$$

where the integration region T means the trapped particle region: $v_\parallel < \varepsilon_h^{1/2} v_\perp$. In view of eq.(8), the quasi-linear fluxes corresponding to eqs.(4) and (7) may be written in the neoclasical expressions:

$$\Gamma = n\sum_k \left|\frac{c\tilde{E}_\theta}{B}\right|_k^2 \left\{-\left(1-\frac{\bar{\omega}}{\omega_{*e}}\right)T_0\frac{n'}{n} - \left(T_1 - \frac{3}{2}T_0\right)\frac{T'}{T}\right\} \tag{37}$$

$$Q = nT\sum_k \left|\frac{c\tilde{E}_\theta}{B}\right|_k^2 \left\{-\left(1-\frac{\bar{\omega}}{\omega_{*e}}\right)T_1\frac{n'}{n} - \left(T_2 - \frac{3}{2}T_1\right)\frac{T'}{T}\right\} \tag{38}$$

where T_j has been defined by

$$T_j = \int_T d^3v \frac{\nu_{eff}}{(\overline{\omega}_r - \omega_D)^2 + \nu_{eff}^2} F_M \overline{E}^j \tag{39}$$

From the coefficent of $-n'$ in eq.(37), by making use of eqs.(14) and (20), the diffusion coefficent is expressed by

$$D_\perp = \sum_k \left|\frac{c\tilde{E}_\theta}{B}\right|_k^2 \int_{-\infty}^{\infty} S(\bar{\omega})\left(1-\frac{\bar{\omega}}{\omega_{*e}}\right)T_0 d\bar{\omega} \tag{40}$$

From the coefficient of $-nT'$ in eq.(38), the heat diffussivity is given by

$$\chi_e = \sum_k \left|\frac{c\tilde{E}_\theta}{B}\right|_k^2 \int_{-\infty}^{\infty} S(\bar{\omega})\left(T_2 - \frac{3}{2}T_1\right)d\bar{\omega} \tag{41}$$

For the sake of simplicity, we apply the same approximation as used in section 2: $\omega_D = \hat{\omega}_D \overline{E}$. In this case, eq.(39) is rewritten in the form

$$T_j = \sqrt{\varepsilon_h}\,\nu_{eff0}\int_0^\infty dE \frac{E^{j-1}e^{-E}}{(\bar{\omega} - \omega_D E)^2 + \nu_{eff0}^2 E^{-3}} \tag{42}$$

where $\nu_{effo} = \nu_o/\varepsilon_h$ is the effctive collisin frequency at thermal velocity. When $\nu_{eff} \gg \omega_D$, the moment integral (42) may be approximated by

$$T_j = \frac{\sqrt{\varepsilon_h}}{\nu_{eff0}}\int_0^\infty dE E^{j+2}e^{-E} \tag{43}$$

In particular, from eq.(43), we have $T_o = 2\varepsilon_h^{1/2}/\nu_{effo}$, $T_1 = 3T_o$ and $T_2 = 4T_1$.

If we assume the cut-off type frequency spectrum as used in section 2, from eq.(40), the diffusion coefficient becomes

$$D_\perp = 2\sum_k \left|\frac{c\tilde{E}_\theta}{B}\right|_k^2 \frac{\varepsilon_h^{3/2}}{\nu_0} \tag{44}$$

By the same manner, the heat diffusivity becomes

$$\chi_e = 15\sum_k \left|\frac{c\tilde{E}_\theta}{B}\right|_k^2 \frac{\varepsilon_h^{3/2}}{\nu_0} \tag{45}$$

In view of the relation (20), if we apply the mixing length relation $|e\tilde{\phi}T| = (k_\perp L)^{-1}$ with $L^2 = L_n L_T$, eq.(44) can be written as

$$D_\perp = \frac{\varepsilon_h^{3/2}\omega_*^2 \eta_e}{\nu_0 k_\perp^2} \tag{46}$$

It is interesting to note that the diffusion coefficient (46) can be expressed by the discrete eigenvalue of the dissipative trapped electron mode (DTEM) [13].

The perturbed ion density is given by

$$\tilde{n}_i = \left(-1 + \int d^3v \frac{\bar{\omega} - \omega_{*Ti}}{\bar{\omega} - \omega_{Di} - k_\parallel v_\parallel} F_M\right)\frac{e\tilde{\phi}}{T_i} n \simeq \frac{\omega_{*e}}{\bar{\omega}}\frac{e\tilde{\phi}}{T_i} n \tag{47}$$

For the trapped electron density, we have

$$\tilde{n}_e = \left(1 - \int d^3v \frac{\bar{\omega} - \omega_{*Te}}{\bar{\omega} - \omega_{De} + i\nu_{eff}} F_M\right)\frac{e\tilde{\phi}}{T_e} n \tag{48}$$

The quasi-neutrality condition, $\check{n}_e = \check{n}_i$, yields the dispersion relation

$$D_{es} = 1 - \frac{\omega_{*e}}{\bar{\omega}} - \int d^3v \frac{\bar{\omega} - \omega_{*Te}}{\bar{\omega} - \omega_{De} + i\nu_{eff}} F_M = 0 \tag{49}$$

The imaginary part of the integral in eq.(49) is equivalent to the normalized flux ϕ_0 defined by eq.(5). Making use of the dispersion relation, which is also equivalent to the ambipolarity relation, we have

$$\phi_0(k, \bar{\omega}) = \frac{\gamma}{\bar{\omega}_r^2 + \gamma^2} \tag{50}$$

where $\omega = \bar{\omega}_r + i\gamma$ is the discrte eigenvalue determined by eq.(49). Introducing eq.(50) into eq.(4), applying the mixing length relation and assuming $\omega_r \simeq \omega_*$, the familiar formula for the diffusion coefficient is obtained:

$$D_\perp = \frac{\omega_{*e}^2}{k_\perp^2}\frac{\gamma}{\omega_{*e}^2+\gamma^2} \cong \frac{\gamma}{k_\perp^2} \quad (51)$$

The approximate growth rate determined from the dispersion relation (49) may be given by $\gamma \cong \varepsilon_h^{3/2}\omega_*^2\eta_e/\nu$[13]. Substitution of this approximation into eq.(51), we have eq.(46).

Equation (46) may be written in the gyro-Bohm form:

$$D_\perp = \chi_{io}\frac{v_i\varepsilon_h^{3/2}}{2\nu_0 L_n} \quad (52)$$

where $\chi_{io}=v_i\rho_i^2/L_T$ is the ion thermal diffusivity obtained in section 2. The diffusion coefficient induced by the dissipative trapped electron mode given by eq.(46) has been applied for the interpretation of experimental results for several kind of discharges in the CHS Heliotron[14]. Due to the factor L_n^{-1} in eq.(52), χ_e tends to zero at the peak point, n'=0, near the periphery, which is the one of the characteristics of the CHS discharges[9]. Since the experimentally observed χ_e does not show such behavior, eq.(52) or eq.(46) alone may not apply to the interpretation of the experimental phenomena.

Let us consider the opposite case of the collisionless limit. Applying the formula

$$\lim_{\nu_{eff}\to 0}\frac{\nu_{eff}}{\nu_{eff}^2+(\bar{\omega}-\omega_D)^2} = \pi\delta(\bar{\omega}-\omega_D) \quad (53)$$

for eq.(39), we have

$$T_j = \frac{\pi\sqrt{\varepsilon_h}}{\omega_D}\left(\frac{\bar{\omega}}{\omega_D}\right)^{j+1/2}\exp\left(-\frac{\bar{\omega}}{\omega_D}\right) \quad (54)$$

Introducing eq.(54) into eq.(41), we have

$$\chi_e = \sum_k\left|\frac{c\tilde{E}_\theta}{B}\right|_k^2\frac{\pi\sqrt{\varepsilon_h}}{2\omega_s}\left(I_2-\frac{3}{2}I_1\right) \quad (55)$$

where I_j has been defined by eq.(21). Applying the mixing length approximation with $k_\perp\rho_i \cong 0.1$, from eq.(55), we have the electron heat diffusivity in term of the modified reduced gyro-Bohm coefficient in the form

$$\chi_e = \frac{10\pi\sqrt{\pi}}{32\tau}\sqrt{\varepsilon_h}\chi_{i0} \quad (56)$$

where $\tau=T_e/T_i$. Since the numerical coefficent in eq.(56) is approximately equal to unity, the electron heat diffusivity induced by the collisionless trapped electrons given by eq.(56) is approximately equal to $\varepsilon_h^{1/2}\chi_{i/\tau}$.

Applying eq.(11) for ion and electron temperatures, the profile of χ_e given by eq.(56) are shown by a surface graphics in Fig. 3 for various values of the electron temperature profile parameter β_{Te}. In this case too, the numerical coefficient and $(v_i\rho_i^2/a)_0$ in eq.(56) have been assumed to be unity. The profile of χ_e shown in Fig. 3 seems to be similar to the experimental one shown in Fig.2, although the value is smaller than χ_i by $\varepsilon_h^{1/2}/\tau$.

If we apply eq.(25) for passing electrons, neglecting the electron transit frequency $k_{\parallel}v_{\parallel} \to 0$, and add the trapped electron contribution given by eq.(55), since the trapped electron contribution may approximately cancel as in the case of ion, we have a similar simple formula

$$\chi_e \cong \frac{\chi_{i0}}{\tau} \qquad (57)$$

In this case, the electron heat diffusivity shows similar (smaller by $1/\tau$) behavior as the ion heat diffusivity shown in Figs.1 and 2. which seem to be consistent with the experimental results.

§5. Summary

Assuming the existence of electrostatic turbulence or scalar potential fluctuations, $\tilde{\phi}$, the quasi-linear cross field particle and heat fluxes induced by the curvature drift resonance and transit resonance have been evaluated in the CHS helical system. The radial electric field makes the Doppler frequency shift which makes no contribution to the cross field fluxes when the frequency spectrum of the fluctuations is symmetric. In other words, the electric field term disappears in the anomaluos fluxes when integrated over the resonance continuum with respect to the frequency. Due to the curvature drift resonance, the fluxes have the curvature term B'/B which contributes to inward transport.

From the coefficient of T', the ion heat diffusivity χ_i has been derived in the simple form as given by eq.(27) which increases toward the periphery as experimentally observed in the CHS and tokamaks[1] discharges.

The quasi-linear fluxes induced by the transit resonance continuum have also been evaluated for passing particles as in Ref.(8), and found that the transit resonance continuum contribution for electrons is negligiblly smaller than the curvature drift resonace contribution.

The curvature drift resonance continuum contribution to fluxes for trapped particles has also been calculated, and the similar simple result for the electron heat diffusivity as given by eq.(56) was obtained. Although this result is smaller by the factor $\varepsilon_h^{1/2}$ than χ_i, it seems more suitable for the interpretation of experimental results as compared with the one induced by dissipative trapped electrons.

When the curvature drift resonance continuum contribution is applied for electron flux neglecting the transit frequency, the trapped particle effect is cancelled out, and the similar simple formula has been obtained as given by eq.(57). This coefficient may be applicable to interpretation of experimental results. There is, however, theoretical difficulty in the treatment of electron transit frequency which may be too large to neglect in usual situations. To compare with experimental obserbations, the anomalous resultsas well as neoclassical theory have to be taken into account because the asymmetric neoclassical effect may not be neglected in the toroidal-helical configuration.

Acknowledgement

The author would like to thank Prof.M.Okamoto for supporting this study. He is grateful to Dr. H.Sanuki, Dr.N.Nakajima and Dr. K.Watanabe for providing information, and many conversations. This study was a joint research effort with the National Institute for Fusion Science.

References

(1) H.Shirai, T.Hirayama, Y.Koide, M.Azumi, D.R. Mikelsen,S.D.Scott, Ion Temperature Profile Simulation of JT-60 and TFTR Plasmas with Ion Temperature Gradient Mode, submitted to Nucl. Fusion.

(2) H.Iguchi, et. al.,Proceeding 1992 Int. Conf. Plasma Physics, Insbruck.

(3) N.G.Van Kampen and B.V.Felderhof,*Theoretical Methods in Plasma*

Physics (translated into Japanese by M. Nishida) Kinokuniya, Tokyo p.153,1973.
(4) K.M.Case and P.F.Zweifel, *Linear Transport Theory*, Addison -Wesley, New York, 1967.
(5) T.Yamagishi, *Cross Field Energy Flux due to Ion Temperature Gradient Mode in a Tokamak*, US-Japan Workshop on η_i-mode and turbulent transport, University of Texas, 1993.
(6) T.Yamagishi,Report NIFS-214(1993).
(7) T.Antonsen, B.Coppi, R.Englade, Nucl.Fusion,**19**(1979)641.
(8) K.C.Shaing, Phys.Fluids,**31**(1988)2249.
(9) H.Sanuki et. al., J.Phys.Soc. Jpn.**60**(1992)3698.
(10) F.Romanelli, Phys.Fluids, **B1**(1989)1018.
(11) H.Sugama,M.Wakatani,Phys.Fluids, **B3**(1991)1110.
(12) H.Nordman,V.P.Pavlenko,J.Wieland,Phys.Fluids **B5**(1993)402.
(13) B.B.Kadomtsev,O.P.Pogutze,Nucl.Fusion **11**(1971)67.
(14) K.Yamazaki,T.Amano,Nucl.Fusion **32**(1992)633.

Figures Captions

Fig.1: Radial profiles of ion heat diffusivity χ_i given by eq.(27) for various values of ion temperature profile parameter β_{Ti}.

Fig.2: Comparison of ion heat diffusivity χ_i given by eq.(27) with experimental values denoted by χ_{iexp} for low and high density discharges in CHS Torsatron.

Fig.3: Radial profiles of electron heat diffusivity χ_e induced by trapped electrons given by eq.(56) for various values of electron temperature profile parameter β_{Te}.

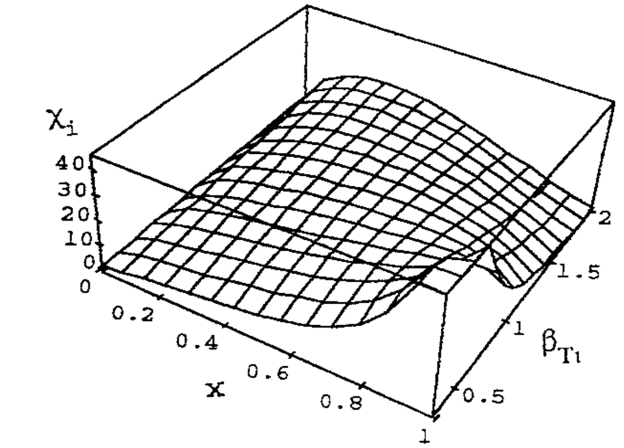

Fig.1

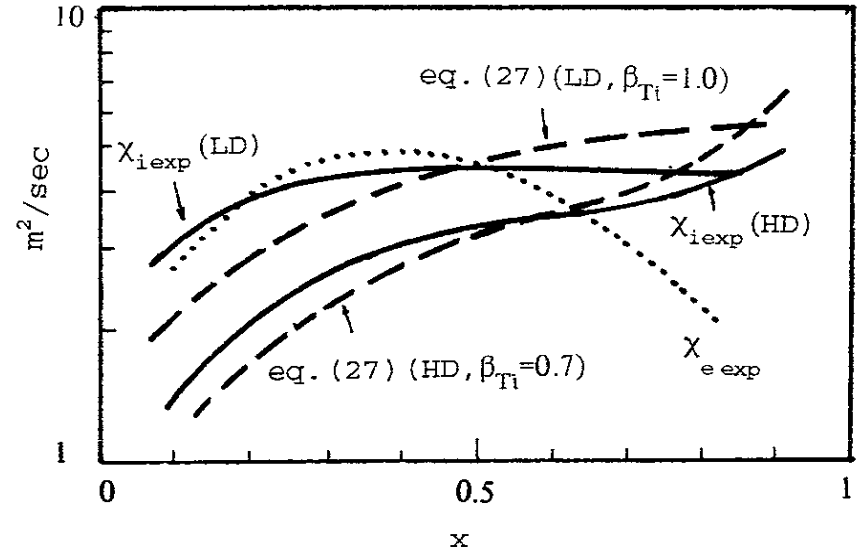

Fig.2

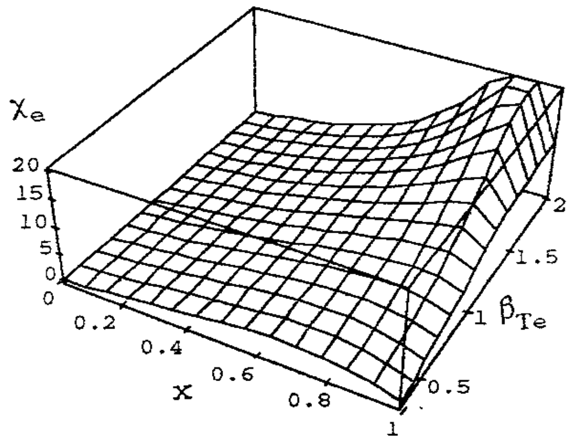

Fig.3

Recent Issues of NIFS Series

NIFS-181 T. Watari, R. Kumazawa, T. Seki, Y. Yasaka, A. Ando, Y. Oka,O. Kaneko, K. Adati, R. Akiyama, Y. Hamada, S. Hidekuma, S. Hirokura, K. Ida, K. Kawahata, T. Kawamoto, Y. Kawasumi, S. Kitagawa, M. Kojima, T. Kuroda, K. Masai, S. Morita, K. Narihara, Y. Ogawa, K. Ohkubo, S. Okajima, T. Ozaki, M. Sakamoto, M. Sasao, K. Sato, K. N. Sato, F.Shimpo, H. Takahashi, S. Tanahasi, Y. Taniguchi, K. Toi, T. Tsuzuki and M. Ono, *The New Features of Ion Bernstein Wave Heating in JIPP T-IIU Tokamak* ;Sep, 1992

NIFS-182 K. Itoh, H. Sanuki and S.-I. Itoh, *Effect of Alpha Particles on Radial Electric Field Structure in Torsatron / Heliotron Reactor*; Sep. 1992

NIFS-183 S. Morimoto, M. Sato, H. Yamada, H. Ji, S. Okamura, S. Kubo, O. Motojima, M. Murakami, T. C. Jernigan, T. S. Bigelow, A. C. England, R. S. Isler, J. F. Lyon, C. H. Ma, D. A. Rasmussen, C. R. Schaich, J. B. Wilgen and J. L. Yarber, *Long Pulse Discharges Sustained by Second Harmonic Electron Cyclotron Heating Using a 35GH$_Z$ Gyrotron in the Advanced Toroidal Facility*; Sep. 1992

NIFS-184 S. Okamura, K. Hanatani, K. Nishimura, R. Akiyama, T. Amano, H. Arimoto, M. Fujiwara, M. Hosokawa, K. Ida, H. Idei, H. Iguchi, O. Kaneko, T. Kawamoto, S. Kubo, R. Kumazawa, K. Matsuoka, S. Morita, O. Motojima, T. Mutoh, N. Nakajima, N. Noda, M. Okamoto, T. Ozaki, A. Sagara, S. Sakakibara, H. Sanuki, T. Seki, T. Shoji, F. Shimbo, C. Takahashi, Y. Takeiri, Y. Takita, K. Toi, K. Tsumori, M. Ueda, T. Watari, H. Yamada and I. Yamada, *Heating Experiments Using Neutral Beams with Variable Injection Angle and ICRF Waves in CHS* ; Sep. 1992

NIFS-185 H. Yamada, S. Morita, K. Ida, S. Okamura, H. Iguchi, S. Sakakibara, K. Nishimura, R. Akiyama, H. Arimoto, M. Fujiwara, K. Hanatani, S. P. Hirshman, K. Ichiguchi, H. Idei, O. Kaneko, T. Kawamoto, S. Kubo, D. K. Lee, K. Matsuoka, O, Motojima, T. Ozaki, V. D. Pustovitov, A. Sagara, H. Sanuki, T. Shoji, C. Takahashi, Y. Takeiri, Y. Takita, S. Tanahashi, J. Todoroki, K. Toi, K. Tsumori, M. Ueda and I. Yamada, *MHD and Confinement Characteristics in the High-β Regime on the CHS Low-Aspect-Ratio Heliotron / Torsatron* ; Sep. 1992

NIFS-186 S. Morita, H. Yamada, H. Iguchi, K. Adati, R. Akiyama, H. Arimoto, M. Fujiwara, Y. Hamada, K. Ida, H. Idei, O. Kaneko, K. Kawahata, T. Kawamoto, S. Kubo, R. Kumazawa, K. Matsuoka, T. Morisaki, K. Nishimura, S. Okamura, T. Ozaki, T. Seki, M. Sakurai, S, Sakakibara, A. Sagara, C. Takahashi, Y. Takeiri, H. Takenaga, Y. Takita, K. Toi, K. Tsumori, K. Uchino, M. Ueda, T. Watari, I. Yamada, *A Role of Neutral Hydrogen in CHS Plasmas with Reheat* *and Collapse and Comparison with JIPP T-IIU Tokamak Plasmas* ; Sep. 1992

NIFS-187 K. Ioth, S.-I. Itoh, A. Fukuyama, M. Yagi and M. Azumi, *Model of the L-Mode Confinement in Tokamaks* ; Sep. 1992

NIFS-188 K. Itoh, A. Fukuyama and S.-I. Itoh, *Beta-Limiting Phenomena in High-Aspect-Ratio Toroidal Helical Plasmas*; Oct. 1992

NIFS-189 K. Itoh, S. -I. Itoh and A. Fukuyama, *Cross Field Ion Motion at Sawtooth Crash* ; Oct. 1992

NIFS-190 N. Noda, Y. Kubota, A. Sagara, N. Ohyabu, K. Akaishi, H. Ji, O. Motojima, M. Hashiba, I. Fujita, T. Hino, T. Yamashina, T. Matsuda, T. Sogabe, T. Matsumoto, K. Kuroda, S. Yamazaki, H. Ise, J. Adachi and T. Suzuki, *Design Study on Divertor Plates of Large Helical Device (LHD)* ; Oct. 1992

NIFS-191 Y. Kondoh, Y. Hosaka and K. Ishii, *Kernel Optimum Nearly-Analytical Discretization (KOND) Algorithm Applied to Parabolic and Hyperbolic Equations* : Oct. 1992

NIFS-192 K. Itoh, M. Yagi, S.-I. Itoh, A. Fukuyama and M. Azumi, *L-Mode Confinement Model Based on Transport-MHD Theory in Tokamaks* ; Oct. 1992

NIFS-193 T. Watari, *Review of Japanese Results on Heating and Current Drive* ; Oct. 1992

NIFS-194 Y. Kondoh, *Eigenfunction for Dissipative Dynamics Operator and Attractor of Dissipative Structure* ; Oct. 1992

NIFS-195 T. Watanabe, H. Oya, K. Watanabe and T. Sato, *Comprehensive Simulation Study on Local and Global Development of Auroral Arcs and Field-Aligned Potentials* ; Oct. 1992

NIFS-196 T. Mori, K. Akaishi, Y. Kubota, O. Motojima, M. Mushiaki, Y. Funato and Y. Hanaoka, *Pumping Experiment of Water on B and* LaB_6 *Films with Electron Beam Evaporator* ; Oct., 1992

NIFS-197 T. Kato and K. Masai, *X-ray Spectra from Hinotori Satellite and Suprathermal Electrons* ; Oct. 1992

NIFS-198 K. Toi, S. Okamura, H. Iguchi, H. Yamada, S. Morita, S. Sakakibara, K. Ida, K. Nishimura, K. Matsuoka, R. Akiyama, H. Arimoto, M. Fujiwara, M. Hosokawa, H. Idei, O. Kaneko, S. Kubo, A. Sagara, C. Takahashi, Y. Takeiri, Y. Takita, K. Tsumori, I. Yamada and H. Zushi, *Formation of H-mode Like Transport Barrier in the CHS*

Heliotron / Torsatron ; Oct. 1992

NIFS-199 M. Tanaka, *A Kinetic Simulation of Low-Frequency Electromagnetic Phenomena in Inhomogeneous Plasmas of Three-Dimensions* ; Nov. 1992

NIFS-200 K. Itoh, S.-I. Itoh, H. Sanuki and A. Fukuyama, *Roles of Electric Field on Toroidal Magnetic Confinement*, Nov. 1992

NIFS-201 G. Gnudi and T. Hatori, *Hamiltonian for the Toroidal Helical Magnetic Field Lines in the Vacuum*; Nov. 1992

NIFS-202 K. Itoh, S.-I. Itoh and A. Fukuyama, *Physics of Transport Phenomena in Magnetic Confinement Plasmas*; Dec. 1992

NIFS-203 Y. Hamada, Y. Kawasumi, H. Iguchi, A. Fujisawa, Y. Abe and M. Takahashi, *Mesh Effect in a Parallel Plate Analyzer*; Dec. 1992

NIFS-204 T. Okada and H. Tazawa, *Two-Stream Instability for a Light Ion Beam -Plasma System with External Magnetic Field;* Dec. 1992

NIFS-205 M. Osakabe, S. Itoh, Y. Gotoh, M. Sasao and J. Fujita, *A Compact Neutron Counter Telescope with Thick Radiator (Cotetra) for Fusion Experiment*; Jan. 1993

NIFS-206 T. Yabe and F. Xiao, *Tracking Sharp Interface of Two Fluids by the CIP (Cubic-Interpolated Propagation) Scheme*, Jan. 1993

NIFS-207 A. Kageyama, K. Watanabe and T. Sato, *Simulation Study of MHD Dynamo : Convection in a Rotating Spherical Shell*; Feb. 1993

NIFS-208 M. Okamoto and S. Murakami, *Plasma Heating in Toroidal Systems*; Feb. 1993

NIFS-209 K. Masai, *Density Dependence of Line Intensities and Application to Plasma Diagnostics*; Feb. 1993

NIFS-210 K. Ohkubo, M. Hosokawa, S. Kubo, M. Sato, Y. Takita and T. Kuroda, *R&D of Transmission Lines for ECH System* ; Feb. 1993

NIFS-211 A. A. Shishkin, K. Y. Watanabe, K. Yamazaki, O. Motojima, D. L. Grekov, M. S. Smirnova and A. V. Zolotukhin, *Some Features of Particle Orbit Behavior in LHD Configurations*; Mar. 1993

NIFS-212 Y. Kondoh, Y. Hosaka and J.-L. Liang, *Demonstration for Novel Self-organization Theory by Three-Dimensional Magnetohydrodynamic Simulation*; Mar. 1993

NIFS-213 K. Itoh, H. Sanuki and S.-I. Itoh, *Thermal and Electric Oscillation Driven by Orbit Loss in Helical Systems*; Mar. 1993

NIFS-214 T. Yamagishi, *Effect of Continuous Eigenvalue Spectrum on Plasma Transport in Toroidal Systems*; Mar. 1993

NIFS-215 K. Ida, K. Itoh, S.-I.Itoh, Y. Miura, JFT-2M Group and A. Fukuyama, *Thickness of the Layer of Strong Radial Electric Field in JFT-2M H-mode Plasmas*; Apr. 1993

NIFS-216 M. Yagi, K. Itoh, S.-I. Itoh, A. Fukuyama and M. Azumi, *Analysis of Current Diffusive Ballooning Mode*; Apr. 1993

NIFS-217 J. Guasp, K. Yamazaki and O. Motojima, *Particle Orbit Analysis for LHD Helical Axis Configurations* ; Apr. 1993

NIFS-218 T. Yabe, T. Ito and M. Okazaki, *Holography Machine HORN-1 for Computer-aided Retrieve of Virtual Three-dimensional Image* ; Apr. 1993

NIFS-219 K. Itoh, S.-I. Itoh, A. Fukuyama, M. Yagi and M. Azumi, *Self-sustained Turbulence and L-Mode Confinement in Toroidal Plasmas* ; Apr. 1993

NIFS-220 T. Watari, R. Kumazawa, T. Mutoh, T. Seki, K. Nishimura and F. Shimpo, *Applications of Non-resonant RF Forces to Improvement of Tokamak Reactor Performances Part I: Application of Ponderomotive Force* ; May 1993

NIFS-221 S.-I. Itoh, K. Itoh, and A. Fukuyama, *ELMy-H mode as Limit Cycle and Transient Responses of H-modes in Tokamaks* ; May 1993

NIFS-222 H. Hojo, M. Inutake, M. Ichimura, R. Katsumata and T. Watanabe, *Interchange Stability Criteria for Anisotropic Central-Cell Plasmas in the Tandem Mirror GAMMA 10 ;* May 1993

NIFS-223 K. Itoh, S.-I. Itoh, M. Yagi, A. Fukuyama and M. Azumi, *Theory of Pseudo-Classical Confinement and Transmutation to L-Mode;* May 1993

NIFS-224 M. Tanaka, *HIDENEK: An Implicit Particle Simulation of Kinetic-MHD Phenomena in Three-Dimensional Plasmas;* May 1993

NIFS-225 H. Hojo and T. Hatori, *Bounce Resonance Heating and Transport in a Magnetic Mirror;* May 1993

NIFS-226 S.-I. Iton, K. Itoh, A. Fukuyama, M. Yagi, *Theory of Anomalous Transport in H-Mode Plasmas;* May 1993